Supramolecular associates of *para*-aminobenzoic acid with N- and N,O-heterocyclic molecules†

Brian Moulton,[a] Brian S. Luisi,[a] Marina S. Fonari,*[b] Stepan S. Basok,[c] Eduard V. Ganin[d] and Victor Ch. Kravtsov[b]

Received (in Montpellier, France) 13th December 2006, Accepted 29th January 2007
First published as an Advance Article on the web 26th February 2007
DOI: 10.1039/b618207k

A series of novel supramolecular multicomponent complexes of *para*-aminobenzoic acid (PABA) with N-containing cyclic molecules and aza-crown ethers, $(H_2PPz)\cdot(PABA)_2\cdot 2H_2O$ (**1**), $(H_2teta)\cdot(PABA)_2\cdot H_2O$ (**2**), $(H_2cyclen)\cdot(PABA)_2\cdot 2H_2O$ (**3**), $(H_2$-diazonia-12C4$)\cdot(PABA)_2\cdot 2H_2O$ (**4**), (H-azonia-18C6$)\cdot(PABA)\cdot 3H_2O$ (**5**) (PPz = piperazine, teta = *meso*-5,7,7,12,12,14-hexamethyl-1,4,8,11-tetraazacyclotetradecane, cyclen = 1,4,7,10-tetraazacyclododecane, diaza-12-crown-4 = 1,7-dioxa-4,10-diazacyclododecane and aza-18-crown-6 = 1,4,7,10,13-pentaoxa-16-azacyclooctadecane) has been synthesized. Crystallographic studies reveal that all complexes are organic salts formed due to the proton transfer from the carboxylic group of PABA to the amino group of the macrocycle, and thus are comprised of PABA anion, macrocyclic mono- or dication and a variable number of water molecules. In all complexes the cations and anions are associated *via* $(H_2N^+)NH\cdots O(COO^-)$ charge-assisted hydrogen bonds. The number of PABA involved in the complex equals to the number of N-protonated binding sites in the cyclic molecule. Water molecules play a significant role in the formation of the supramolecular architecture.

Introduction

The *para*-aminobenzoic acid (PABA) molecule as well as *para*-aminobenzoate salts are known for their role in biological processes[1] and are well suited for use in supramolecular syntheses based on hydrogen bonding interactions with a variety of organic acids and bases. The presence of favorably arranged carboxylic and amino groups in PABA affords the generation of advantageous hydrogen-bonded arrays because these functional groups can form predictable patterns useful for constructing a wide range of supramolecular assemblies. This property was recognized by Etter and Frankenbach[2] as a possible tool for promoting co-crystallization with the aim of designing acentric organic materials. Since the first PABA structural determination by Alleaume *et al.* in 1966,[3] a number of works devoted to PABA complexes have appeared; however, only three complexes between a neutral PABA molecule and 18-membered O-containing macrocycles, 18-crown-6[4] and *cis*-isomers of dicyclohexano-18-crown-6,[5] have been previously reported. Moreover, only two other studies describe ionic complexes of the *para*-aminobenzoate anion with protonated aza-containing macrocycles (cyclam, 1,4,8,11-tetraazacyclotetradecane,[6] and aza-12-crown-4[7]).

A survey of the Cambridge Structural Database[8] (version 5.27, update August 2006) revealed two known PABA polymorphs: in the α-form, molecules form chains *via* alternating carboxyl–carboxyl and amine–carboxyl homo- and heterosynthons,[9] while only amine–carboxyl heterosynthons are responsible for the 3D association of PABA molecules in the β-polymorph.[10] PABA is known to be neutral, cationic or anionic in its complexes. Complexes of PABA with such molecules as 4-nitropyridine *N*-oxide (1 : 1), 1,3,5-trinitrobenzene, urea, 2-carboxyphenoxyacetic acid, 4,4′-bipyridyl *N*,*N*-dioxide, carbamazepine, 4,4′-bipyridine, 2,2′-bipyridine[11–18] represent neutral adducts. Lynch and McClenaghan[19] investigated the influence of the pK_a values on the formation of either neutral-component co-crystals or proton-transfer complexes. In a small number of multicomponent compounds, the carboxylic group of PABA (pK_a = 2.38) protonates the amino group of a Lewis base, *e.g.*, diethylamine (1 : 1)[20] or 2-aminopyrimidine (2 : 1).[21] On the other hand, the amino group of PABA is reported to be protonated by such acids as 3,5-dinitrosalicylic, 5-sulfosalicylic or fluorosilicic acid.[22–24]

As a part of our ongoing efforts toward the supramolecular synthesis of new multicomponent solids involving active pharmaceutical ingredients (APIs), we carried out the systematic investigation of the interaction of PABA with azaheterocycles having different ring sizes (6, 12, 14, 18 atoms in the ring) and a variable number of basic nitrogen atoms (n = 1, 2, 4) capable of varying degrees of protonation by acidic moieties (in our case PABA). The ionized acid–base pairs,[25] or salts by

[a] *Department of Chemistry, Brown University, Providence, Rhode Island, 02912, USA*
[b] *Institute of Applied Physics, Academy of Sciences of Moldova, Academiei str., 5 MD-2028 Chişinău, R. Moldova. E-mail: kravtsov.xray@phys.asm.md. E-mail: fonari.xray@phys.asm.md; Fax: (+373 22) 725887; Tel: (+373 22) 738154*
[c] *A.V. Bogatsky Physico-Chemical Institute, Lustdorfskaya dorogam, 86, 65080 Odessa, Ukraine*
[d] *Odessa State Environmental University, Lvovskaya str., 15, 65016 Odessa, Ukraine*

† The HTML version of this article has been enhanced with colour images.

definition, are the most common multiple-component systems involving APIs.[26,27] To the best of our knowledge, this contribution is the first systematic study of PABA interaction with cyclic molecules of different size and chemical nature.

Experimental

Synthesis and crystallization

Complexes **1–4** were obtained in a similar way by mixing of the corresponding macrocycle (1 mmol) with PABA (2 mmol) in a water–methanol solution and heating until completely dissolved. Complex **5** was obtained by dissolving of an equimolar (1 mmol) amount of the corresponding macrocycle and PABA in a hot water–methanol solution. Crystals suitable for X-ray structural determination were obtained by recrystallization from a mixture of methanol and ethyl acetate. Initial crystallization products were characterized by elemental analysis. Melting points for co-crystals were determined and are presented in Table 1 along with the melting points for the parent compounds.

1. $C_{18}H_{28}N_4O_6$: Calc.: C, 54.53; H, 7.12; N, 14.13. Found: C, 54.57; H, 7.16; N, 14.10%.

2. $C_{30}H_{52}N_6O_5$: Calc.: C, 62.47; H, 9.09; N, 14.57. Found: C, 62.45; H, 9.13; N, 14.61%.

3. $C_{22}H_{38}N_6O_6$: Calc.: C, 54.76; H, 7.94; N, 17.42. Found: C, 54.78; H, 7.91; N, 17.46%.

4. $C_{22}H_{36}N_4O_8$: Calc.: C, 54.53; H, 7.49; N, 11.56. Found: C, 54.56; H, 7.45; N, 11.53%.

5. $C_{19}H_{38}N_2O_{10}$: Calc.: C, 50.21; H, 8.43; N, 6.16. Found: C, 50.24; H, 8.47; N, 6.19%.

Structure determinations

X-Ray data for all complexes were collected on a Bruker SMART-APEX CCD diffractometer by ω and φ-scan mode at 90 K using graphite-monochromated Mo-Kα radiation. There was no intensity decay. Structure solutions were performed by direct methods (SHELXS-97) and refined by full-matrix least-squares methods on F^2 (SHELXL-97).[28] Lorentz and polarization corrections were applied for diffracted reflections. In addition, the data were corrected for absorption using SADABS.[29] In all complexes non-hydrogen atoms were refined anisotropically. H atoms attached to carbons were included in idealized positions in a riding model with isotropic temperature factors (1.2 times the parent carbon atom temperature factor), whereas those on N and O(water) atoms were found from difference Fourier maps and refined isotropically.

Table 1 Melting points for the starting materials and complexes **1–5**

Complex	Starting materials		Complex
	Mp (L)/°C	Mp (PABA)/°C	Mp/°C
1 (piperazinium)$(PABA)_2 \cdot 2H_2O$	44–45	188–189	189–190
2 $(H_2teta)(PABA)_2 \cdot H_2O$	97–105	188–189	270–271
3 $(H_2cyclen)(PABA)_2 \cdot 2H_2O$	108–113	188–189	206–207
4 (diazonia12C4)$(PABA)_2 \cdot 2H_2O$	56–57	188–189	126–127
5 (azonia18C6)$(PABA) \cdot 3H_2O$	46–50	188–189	111–112

The hydrogen bonding geometry for **1–5** is summarised in Table 2. All the figures were prepared using MERCURY facilities. Displacement ellipsoids are shown with 50% probability level.

Crystal/refinement data

1. $C_{18}H_{28}N_4O_6$: M = 396.44, monoclinic, space group $P2_1/c$, a = 6.5739(13), b = 11.597(2), c = 12.604(3) Å, β = 90.13(3)°, V = 960.9(3) Å^3, Z = 2, D_c = 1.370 g cm^{-3}, μ = 0.104 mm^{-1}, specimen: 0.22 × 0.25 × 0.30 mm, 'T' min/max = 0.74, N_t = 7319, N = 1891, N_o = 1685 (R_{int} = 0.0287), GOF on F^2 = 1.005. Final R indices [$I > 2\sigma(I)$]: $R1$ = 0.0373, $wR2$ = 0.1039; R indices (all data): $R1$ = 0.0420, $wR2$ = 0.1073.

2. $C_{30}H_{52}N_6O_5$: M = 576.78, monoclinic, $C2/c$, a = 19.0506(13), b = 12.1200(9), c = 14.4397(10) Å, β = 107.72(1)°, V = 175.8(4) Å^3, Z = 4, D_c = 1.206 g cm^{-3}, μ = 0.083 mm^{-1}, specimen: 0.25 × 0.25 × 0.20 mm, 'T' min/max = 0.87, N_t = 13 533, N = 3646, N_o = 2940 (R_{int} = 0.0321), GOF on F^2 = 1.006. Final R indices [$I > 2\sigma(I)$]: $R1$ = 0.0484, $wR2$ = 0.1211; R indices (all data): $R1$ = 0.0619, $wR2$ = 0.1283.

3. $C_{22}H_{38}N_6O_6$: M = 482.58, monoclinic, $P2_1$, a = 9.6004(19), b = 11.350(2), c = 12.088(2) Å, β = 111.91(3)°. V = 1222.0(4) Å^3, Z = 2, D_c = 1.311 g cm^{-3}, μ = 0.096 mm^{-1}, specimen: 0.20 × 0.20 × 0.40 mm, 'T' min/max = 0.80. N_t = 9148, N = 4232, N_o = 3939 (R_{int} = 0.0272), GOF on F^2 = 1.009. Final R indices [$I > 2\sigma(I)$]: $R1$ = 0.0366, $wR2$ = 0.0881; R indices (all data): $R1$ = 0.0400, $wR2$ = 0.0906.

4. $C_{22}H_{36}N_4O_8$: M = 484.55 monoclinic, Pc, a = 10.9044(14), b = 9.9475(13), c = 12.1429(15) Å, β = 114.267(2)°, V = 1200.8(3) Å^3, Z = 2, D_c = 1.340 g cm^{-3}, μ = 0.102 mm^{-1}, specimen: 0.10 × 0.40 × 0.40 mm, 'T' min/max = 0.58. N_t = 8749, N = 4343, N_o = 4062 (R_{int} = 0.0267), GOF on F^2 = 1.004. Final R indices [$I > 2\sigma(I)$]: $R1$ = 0.0349, $wR2$ = 0.0800; R indices (all data): $R1$ = 0.0381, $wR2$ = 0.0825.

5. $C_{19}H_{38}N_2O_{10}$: M = 454.51, orthorhombic, $Pca2_1$, a = 24.784(4), b = 9.6757(17), c = 10.0867(18) Å, V = 2418.8(7) Å^3, Z = 4, D_c = 1.248 g cm^{-3}, μ = 0.100 mm^{-1}, specimen: 0.10 × 0.30 × 0.30 mm, 'T' min/max = 0.57, N_t = 12 926, N = 3892, N_o = 3038 (R_{int} = 0.0601), GOF on F^2 = 0.996. Final R indices [$I > 2\sigma(I)$]: $R1$ = 0.0424, $wR2$ = 0.0849, R indices (all data): $R1$ = 0.0575, $wR2$ = 0.0913.

CCDC reference numbers 626905–626909.

For crystallographic data in CIF or other electronic format see DOI: 10.1039/b618207k

Results and discussion

Commercially available PABA, N- and N,O-containing cycles, piperazine, *meso*-5,7,7,12,12,14-hexamethyl-1,4,8,11-tetraazacyclotetradecane (teta), 1,4,7,10-tetraazacyclododecane (cyclen), and azacrown ethers, 1,7-dioxa-4,10-diazacyclododecane (diaza-12-crown-4) and 1,4,7,10,13-pentaoxa-16-azacyclooctadecane

Table 2 Hydrogen bonding geometry in **1–5** (Å, °)

D–H···A	*d*(D–H)	*D*(H···A)	*d*(D···A)	∠(DHA)	Symmetry operation for acceptor
1					
N(1)–H(2N1)···O(1W)	0.89(2)	2.04(2)	2.930(2)	178(2)	$x + 1, -y + \frac{1}{2}, z + \frac{1}{2}$
N(2)–H(1N2)···O(2)	0.92(2)	1.80(2)	2.697(2)	165(2)	$-x + 2, -y + 1, -z$
N(2)–H(2N2)···O(1)	0.95(2)	1.72(2)	2.632(2)	160(2)	x, y, z
O(1W)–H(1W1)···O(1)	0.87(2)	1.95(2)	2.804(2)	168(2)	x, y, z
O(1W)–H(2W1)···O(2)	0.88(2)	1.92(2)	2.789(2)	168(2)	$-x + 2, y - \frac{1}{2}, -z + \frac{1}{2}$
2					
N(1)–H(1N1)···O(2)	0.86(2)	2.07(2)	2.923(2)	170(2)	$x, -y, z - \frac{1}{2}$
N(1)–H(2N1)···O(2)	0.89(2)	2.10(2)	2.988(2)	176(2)	$-x + \frac{1}{2}, y - \frac{1}{2}, -z - \frac{1}{2}$
N(2)–H(1N2)···O(1W)	0.89(2)	2.16(2)	3.040(1)	172(1)	$-x + 1, -y + 1, -z$
N(3)–H(1N3)···N(2)	0.94(2)	2.01(2)	2.790(2)	139(1)	x, y, z
N(3)–H(2N3)···O(1)	0.93(2)	1.78(2)	2.704(2)	171(2)	x, y, z
O(1W)–H(1W)···O(1)	0.93(2)	1.82(2)	2.737(1)	168(2)	$-x + 1, -y + 1, -z$
3					
N(1A)–H(1NA)···O(2W)	0.94(2)	1.99(2)	2.928(3)	176(2)	$x, y - 1, z + 1$
N(1A)–H(2NA)···O(1A)	0.89(3)	2.03(3)	2.911(3)	170(3)	$-x - 1, y - \frac{1}{2}, -z$
N(1B)–H(1NB)···O(2B)	0.94(3)	2.27(3)	3.098(3)	146(2)	$-x - 2, y - \frac{1}{2}, -z - 1$
N(1B)–H(2NB)···O(1W)	0.92(3)	2.14(3)	2.981(3)	152(2)	$-x - 2, y + \frac{1}{2}, -z - 1$
N(3)–H(1N3)···N(4)	0.94(2)	2.29(2)	2.796(3)	113(2)	x, y, z
N(3)–H(1N3)···N(2)	0.94(2)	2.34(2)	2.857(2)	114(2)	x, y, z
N(3)–H(2N3)···O(1B)	0.92(2)	1.82(2)	2.710(2)	164(2)	x, y, z
N(4)–H(1N4)···O(2B)	0.86(2)	2.28(2)	3.116(2)	163(2)	$-x - 1, y - \frac{1}{2}, -z - 1$
N(5)–H(1N5)···O(2A)	0.97(3)	1.71(3)	2.656(2)	165(2)	x, y, z
N(5)–H(1N5)···O(1A)	0.97(3)	2.45(3)	3.146(2)	129(2)	x, y, z
N(5)–H(2N5)···N(2)	0.87(2)	2.37(2)	2.840(3)	114(2)	x, y, z
O(1W)–H(1W1)···O(1B)	0.89(3)	1.98(3)	2.850(2)	166(3)	$-x - 1, y - \frac{1}{2}, -z - 1$
O(1W)–H(2W1)···O(1A)	0.85(3)	1.92(4)	2.753(2)	167(3)	x, y, z
O(2W)–H(1W2)···O(1B)	0.89(3)	1.98(3)	2.869(2)	172(2)	$-x - 1, y + \frac{1}{2}, -z - 1$
O(2W)–H(2W2)···O(2B)	0.91(4)	1.87(4)	2.765(2)	165(3)	x, y, z
4					
N(1A)–H(2NA)···O(1B)	0.84(3)	2.36(3)	3.069(3)	143(2)	$x, -y - 1, z - \frac{1}{2}$
N(1B)–H(1NB)···O(1W)	0.86(3)	2.27(3)	3.105(3)	165(2)	$x - 1, y - 1, z$
N(1B)–H(2NB)···O(2A)	0.88(3)	2.08(3)	2.942(3)	163(2)	$x - 1, -y - 1, z - \frac{1}{2}$
N(3)–H(3A)···O(1W)	0.88(3)	1.93(3)	2.777(2)	162(2)	x, y, z
N(3)–H(3B)···O(1A)	0.90(3)	1.97(3)	2.850(2)	164(2)	x, y, z
N(4)–H(4A)···O(1A)	0.91(2)	2.18(2)	2.993(2)	148(2)	x, y, z
N(4)–H(4B)···O(1B)	0.98(2)	1.66(2)	2.635(2)	169(2)	x, y, z
O(1W)–H(1W1)···O(2B)	0.86(2)	1.87(2)	2.725(2)	172(3)	$x + 1, -y, z + \frac{1}{2}$
O(1W)–H(2W1)···O(2W)	0.87(2)	1.83(2)	2.698(2)	172(3)	x, y, z
O(2W)–H(1W2)···O(2A)	0.86(2)	1.98(2)	2.762(2)	150(2)	x, y, z
O(2W)–H(2W2)···O(1B)	0.87(3)	1.92(3)	2.758(2)	162(4)	$x + 1, y, z$
5					
N(1)–H(1N1)···O(5)	0.88(3)	2.22(3)	3.061(3)	161(3)	$x, y - 1, z + 1$
N(1)–H(2N1)···O(2)	0.90(3)	2.08(3)	2.962(3)	167(3)	$-x + 1, -y, z + \frac{1}{2}$
N(2)–H(2N2)···O(1)	0.86(3)	1.91(3)	2.759(3)	170(3)	x, y, z
N(2)–H(1N2)···O(1W)	0.98(3)	1.90(3)	2.881(3)	171(3)	x, y, z
O(1W)–H(1W1)···O(6)	0.88(6)	1.97(6)	2.838(3)	167(5)	x, y, z
O(1W)–H(2W1)···O(4)	0.83(4)	2.26(4)	3.077(3)	170(4)	x, y, z
O(1W)–H(2W1)···O(3)	0.83(4)	2.54(4)	2.999(3)	116(3)	x, y, z
O(2W)–H(1W2)···O(3W)	0.81(5)	2.04(5)	2.799(3)	156(5)	x, y, z
O(2W)–H(2W2)···O(1W)	0.85(4)	2.09(4)	2.938(3)	172(4)	x, y, z
O(3W)–H(1W3)···O(2W)	0.82(5)	2.11(5)	2.908(3)	164(4)	$-x + \frac{3}{2}, y, z + \frac{1}{2}$
O(3W)–H(2W3)···O(1)	0.80(4)	1.99(4)	2.784(3)	175(4)	x, y, z

(aza-18C6) were chosen for complex formation. The macrocycles gradually increase from 6 to 18 ring atoms, and contain one to four 'anchor positions', namely secondary NH-amino groups capable of being protonated to give a mono-, di-, tri- or tetra-cation.[8] In the complexes described herein, only aza-18C6 is protonated by PABA to a single cation, while all the other macrocycles are doubly protonated to form the dications.

In all five complexes the acidic proton transfer occurs from the carboxylic group of PABA molecule to the amino-group of macrocycle. The crystallographic evidence for this proton transfer is the approximately equal C–O distances in the carboxylate group consistent with the carboxylate anion (the most different values in the same COO^- group are 1.250 and 1.278 Å that correspond to the delocalised C–O bond) and

Fig. 1 ORTEP plot of the compact formula unit in **1**.

unbiased localisation of two hydrogen atoms in the close proximity of macrocyclic nitrogen atoms.

The formula units for five studied complexes **1–5** shown in Figs. 1–5 represent the common view of the hydrated acid–base complexes of the compositions $(H_2L)(PABA)_2 \cdot 2H_2O$ for L = piperazine, cyclen, diaza-12C4 (complexes **1**, **3** and **4**, respectively), $(H_2L)(PABA)_2 \cdot H_2O$ for L = teta (complex **2**), and $(HL)(PABA) \cdot 3H_2O$ for L = aza-18C6 (complex **5**). The hydrogen bonds for **1–5** are listed in Table 2. The ionic components of **1–5** invariably form charge-assisted hydrogen bonds, and the $N(NH_2^+)\cdots O(COO^-)$ distances are the shortest amongst those that sustain the structures. In all materials, the H-bonded complexes form additional hydrogen bonds to water molecules resulting in 3D supramolecular architectures where PABA moieties are involved in both PABA–macrocycle and PABA–PABA interactions. The N–H···O and O–H···O hydrogen bonds provide for intermolecular binding, while N–H···N intramolecular hydrogen bonds were found within $(H_2teta)^{2+}$ and $(H_2cyclen)^{2+}$ dications.

In **1** (Fig. 6(a)) each aminia group is H-bonded to two PABA anions, which act as a bridge between two centrosymmetric piperazinium cations, resulting in a supramolecular chain along [010]. The length of the two hydrogen bonds varies slightly (N···O separations being 2.697 and 2.632 Å), both being the shortest in the structure. The resulting supramolecular synthons are hetero-tetramers corresponding to the $R_4^4(12)$ rings in graph set notation.[30] Furthermore, two inversion center related PABA anions and two water molecules form $R_4^4(20)$ hetero-tetrameric rings, which assemble into corrugated chains *via* shared water molecules (Fig. 6(b)). The combination of these two motifs results in the 3D grid.

In **2** (Fig. 2) the $(H_2teta)^{2+}$ dication resides around an inversion center, and the anion occupies a general position. The acid–base interaction (N···O separations being 2.704(2) Å) is the shortest in the structure; but unlike **1**, only one carboxylate oxygen, O1, participates in the PABA–cycle interaction. Additionally aminia moieties are involved in typical NH···H intramolecular hydrogen bonds that span the cyclic cavity. The other carboxylate oxygen atom, O2, and the amino-group of PABA are involved in NH···O anion–anion self-associated interactions *via* alternating of $R_2^4(8)$ and $R_4^4(32)$ rings, thus generating a negatively charged sheet as shown in Fig. 7(a). The same anionic sheet was reported in the structure $(cyclamH_2)^{2+} \cdot 2(PABA)^- \cdot H_2O$[6] and resembles the association of neutral PABA molecules in its β-polymorph.[10] The $(H_2teta)^{2+}$ cations are linked to the anionic framework *via* direct NH···O hydrogen bonds and additionally *via* intermediate water molecules. The mode of water incorporation in the crystal structure is depicted in Fig. 7(b).

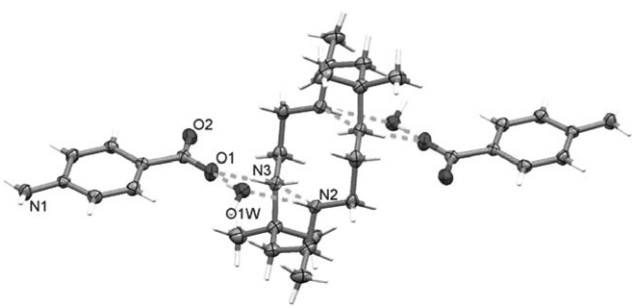

Fig. 2 ORTEP plot of the compact formula unit in **2**.

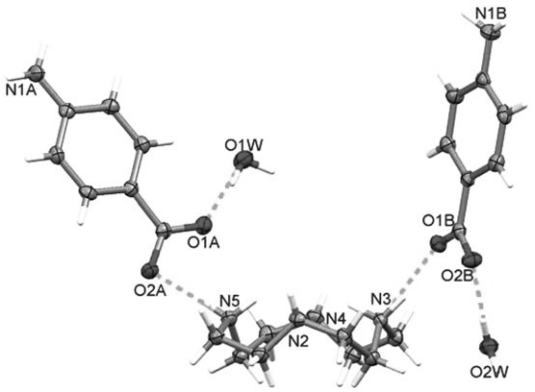

Fig. 3 ORTEP plot of the compact formula unit in **3**.

Complexes **3** and **4** both contain the 12-membered macrocyclic dication, two crystallographically non-equivalent PABA anions (A and B) and two water molecules (Fig. 3 and Fig. 4). Although in the both cycles NH_2^+-aminia centers are separated by the chain $[CH_2CH_2O(NH)CH_2CH_2]$ of the same length, the conformations of the molecules are different, due to the different set of donor, acceptor atoms in the rings and the availability of the short intramolecular $NH^+\cdots N$ interactions in $(H_2cyclen)^{2+}$ (Table 2). This results in different modes of interaction with PABA anions, as it is clearly evident from Fig. 3 and Fig. 4. In **3**, three charged components are held together *via* two single $NH^+\cdots O$ hydrogen bonds, 2.656(2) and 2.710(2) Å, and the anions are in a 'side arrangement',

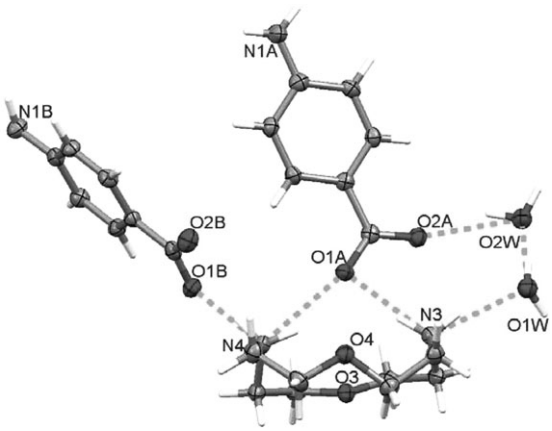

Fig. 4 ORTEP plot of the compact formula unit in **4**.

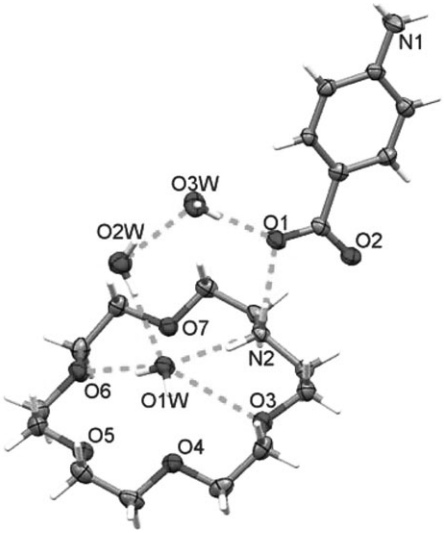

Fig. 5 ORTEP plot of the compact formula unit in **5**.

while in **4** one of the PABA anions acts as a bridge between two cyclic nitrogens, N3 and N4, and thus is arranged just above the cyclic cavity. Further differences are evident from the PABA anions arrangements in the crystals. In complex **3** the PABA-A anions form head-to-tail chains due to the $NH_2\cdots O(COO^-)$ interactions (Fig. 8), which alternate with the PABA-B anions without any direct PABA–PABA H-bonded interactions, and are surrounded by water molecules. The connection of two types of anions occurs *via* 12-membered

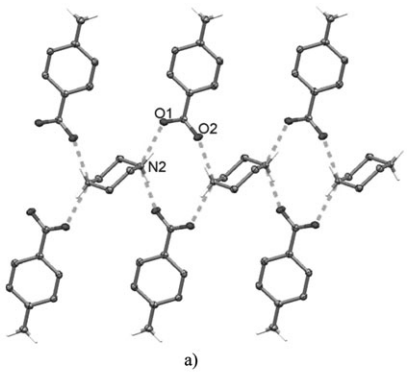

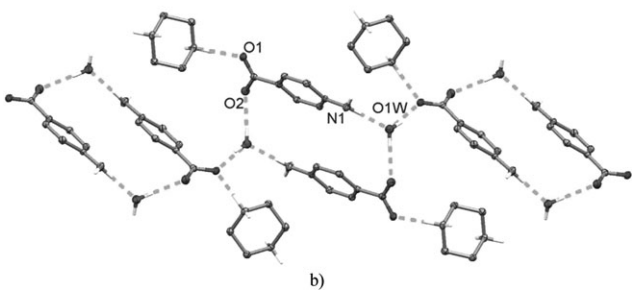

Fig. 6 (a) Fragment of chain combining the opposite-charged components in **1**. (b) Mode of association of PABA anions and water molecules, only few of the piperazinium cations attached to this chain are shown. C-bound H-atoms are omitted for clarity.

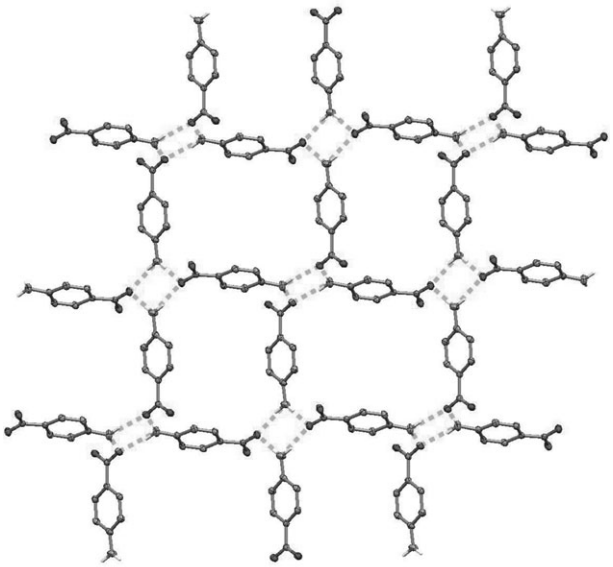

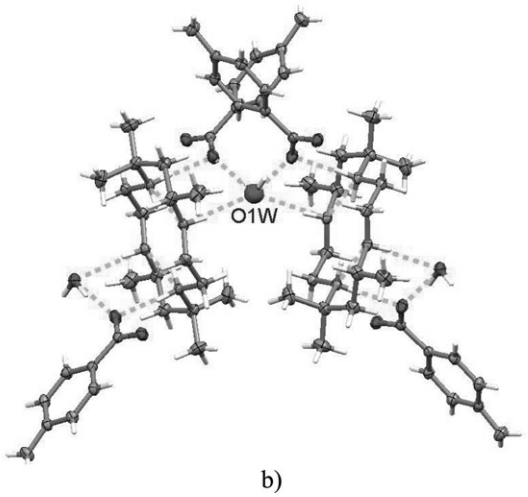

Fig. 7 (a) The negative sheet of PABA anions in **2** sustained by the alternation of $R_2^4(8)$ and $R_4^4(32)$ hydrogen-bonded rings. C-bound H-atoms are omitted for clarity. (b) The mode of water incorporation in the structure.

H-bonded ring and combines two PABA-A anions that belong to the same chain, one PABA-B anion and two different water molecules. It is interesting to note that PABA-B anion appears to be completely hydrated, its carboxylic group and one hydrogen of amino group participate in three $COO^-\cdots O$(water) and one $NH\cdots O$(water) hydrogen bonds.

In **4** six hydrogen bonds of the $NH^+\cdots O^-$ and $OH\cdots O$ types act within the formula unit shown in Fig. 4, while four other bind the formula units into a supramolecular 3D network: translated along [100] direction complexes are combined into chain *via* bridging O2W water molecule (Fig. 9(a)). The amino-group of each of two symmetrically independent PABA anions (A or B), being hydrogen bonded with its counterpart, forms the ABAB head-to-tail chain (Fig. 9(b)), similar to that

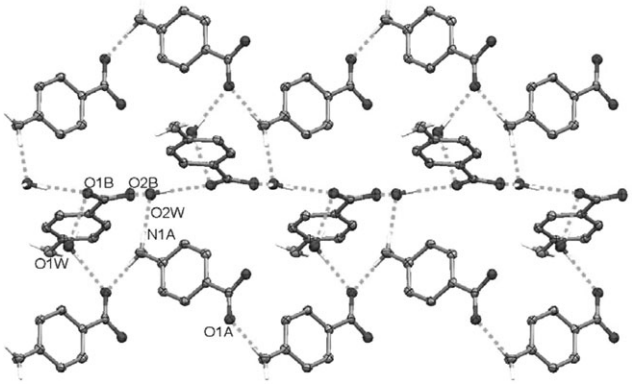

Fig. 8 Fragment of the continuous negative motif in **3** built of the alternative rows of PABA-A and -B anions and water molecules; view down the [100] direction. The $R_5^4(12)$ ring in a conditional 'boat' conformation binds three PABA anions (AAB) and two water molecules. C-bound H-atoms and $[H_2cyclen]^{2+}$ cations are omitted for clarity.

found in **3**. Water molecule O1W unites these two structural motifs into 3D grid.

Contrary to **1–3**, with the point inclusion of water molecules in those structures, in **4** we observe the association of two water molecules into a two-membered O1W···O2W water cluster, the O···O separation being 2.698(2) Å. These water molecules act as double donors and single acceptors, thus only the O1W water molecule interacts with the macrocycle, while the second O2W water molecule bridges carboxylic groups of A and B anions.

Complex **5** stands aside due to only one cyclic aminia binding site, the largest cavity amongst the discussed hetero-

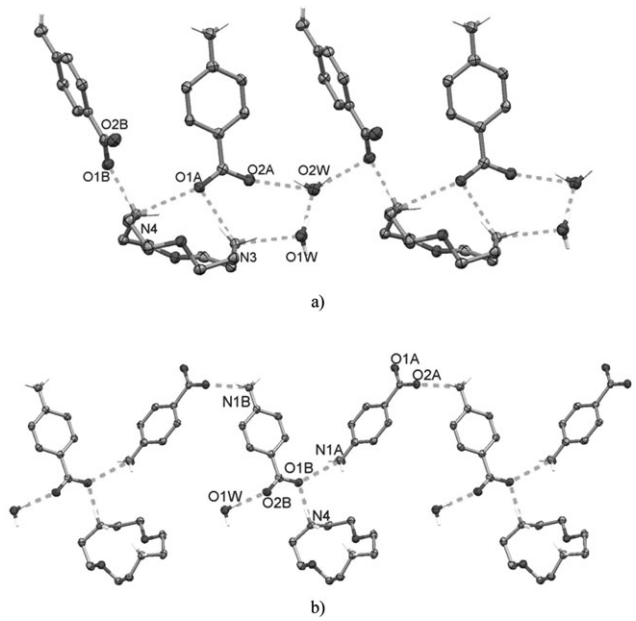

Fig. 9 (a) The hydrogen-bonded chain of complexes **4** developed along [100] direction. (b) The chain of alternating A and B PABA anions running along [001] direction. Only a few of the macrocyclic cations are shown. C-bound H-atoms are omitted for clarity.

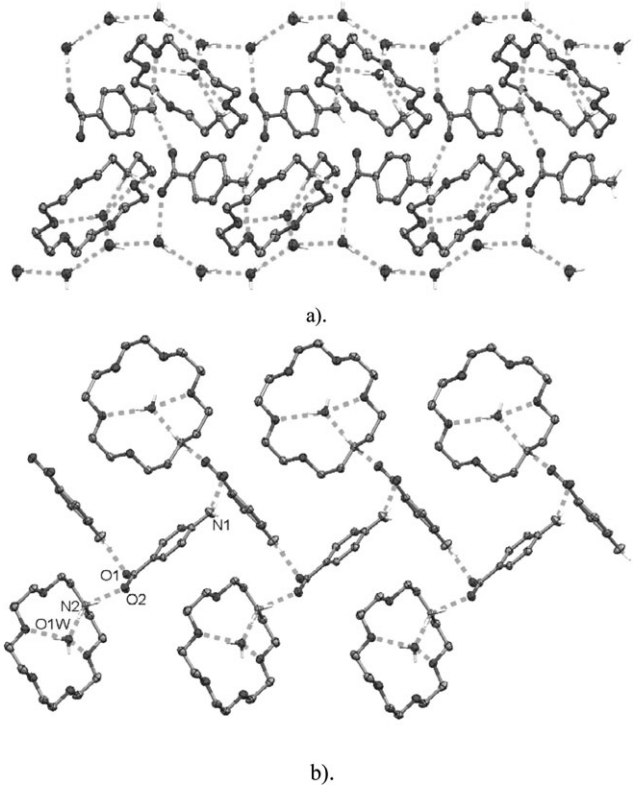

Fig. 10 (a) Fragment of crystal packing in **5** showing the bridging PABA and macrocyclic cation inclusion and water chains, view along [010] direction. (b) Fragment of face-to-tail PABA chain with the macrocyclic cations attached to the PABA carboxylic moiety. C-bound H-atoms are omitted for clarity.

cycles and the richness in a number of included water molecules. Three incorporated water molecules fulfill different structural functions. Water molecule O1W in a perching mode centers the macrocyclic cavity acting as an H-double donor towards macrocyclic oxygens and as an H-acceptor from one of the aminia hydrogens. The displacement of O1W atom from the mean plane of the macrocyclic heteroatoms equals to 0.918 Å. The same O1W water molecule is H-bonded to the next O2W water molecule, which, alternating with O3W, form the continuous water chain in the structure (Fig. 10(a)). The NH_2^+-group of the macrocycle is characterized by the *exo*,*endo*-orientation of its hydrogen atoms, that explains the 1 : 1 ratio of the acid–base associate, where the charged units are bound *via* one single $NH^+\cdots O(COO^-)$ hydrogen bond, N2···O1 2.759(3) Å. This structure is also exceptional by the involvement of PABA amino-group in the interactions with the crown oxygen atom of the macrocylic cavity *via* a conventional NH···O hydrogen bond, N1···O5, 3.061(3) Å and, henceforth, the bridging function of both PABA anion and the macrocyclic cation. The robust motif of PABA···PABA head-to-tail association still exists in this structure, combining anions related by the two-fold screw axis (Fig. 10(b)).

The predominant structural features in complexes **1–5** are the interaction of the PABA carboxylic group with the amino-group of cyclic molecule accompanied by a proton transfer and resulting in either single NH···O hydrogen bond in **1–3**

and **5**, or bifurcated (two-point) hydrogen bond in **4**. Data mining the CSD[8] reveals no examples for cyclen, diaza-12-crown-4 and aza-18-crown-6 complexes with carbonic acids, and thus this contribution represents the first examination of such interactions, with a specific emphasis on the interaction of PABA with these cyclic molecules. Examples of interactions between carbonic acids and teta (Refcodes CUTVOC, CUVNOW, CUVNUC, JAHCOL, HUSRUI, WUXJAA) and piperazine (more than 50 hits), reveal that all adducts are organic salts with the carboxylate group involved in the different modes of interaction with the protonated binding site of the ring. The tetrameric mode of two carboxylic groups and two NH_2^+-aminia centers association found in **1**, is typical for piperazinium adducts (BAKYES, BEXCEM10, BEXDAJ01, BEXDIR01, BOCLIO, RIKBIW, ZEMXOE, ZUGQEX), including the formation of $R_4^4(12)$ heterosynthon (HIHJOX, QIBRUO, VAJWUZ). Surprisingly, no chelate-type interaction, common for carboxylic groups and observed for the *para*-aminobenzoate anion in its cyclam complex[6] and for the salicylate anion in complexes with similar macrocycles,[31] was exhibited here. Typical for 'all O-containing' crown ethers, an interaction with the neutral PABA molecule *via* two conventional NH···O(crown) hydrogen bonds with the PABA amino-group exhibits itself only in complex **5** in the form of a rather weak single subsidiary NH(PABA)···O(crown) interaction.

Excluding **1**, two main motifs of PABA anion self-association are observed: in **3–5** the PABA anions are linked into a head-to-tail chain *via* a single NH···O hydrogen bond; the sheet motif similar to that in β-polymorph of PABA is observed only in **2** and in $(cyclamH_2)^{2+} \cdot 2(PABA)^- \cdot H_2O$.[6]

Water molecules feature different structural functions in the complexes.[32,33] Water point inclusion is registered in **1–3**: in **1** it acts as a double H-donor and single H-acceptor towards three PABA anions and is responsible for their association in the ribbons. Water incorporation in **1** results in a complete violation of any self-association of PABA anions. This situation differs from **2**, where water function, although present, might be considered as a negligible one, adding only a minor component to the binding between the $(H_2teta)^{2+}$ cations and PABA anionic sheet, which is the most ordered and vast fragment of PABA association within **1–5**. The transition from aza-macrocycles to N,O-crown ethers reveals the association of water molecules, acting as a two-membered cluster in **4**, three-membered cluster in bis(1,4,7-trioxa-10-azoniacyclododecane) bis(4-aminobenzoate) trihydrate[7] or as an infinite chain in **5**.

Conclusion

The supramolecular synthesis of the PABA–macrocycle complexes in a water–methanol solution unambiguously leads to the organic hydrated salts. The number of PABA involved in the complex equals to the number of N-protonated binding sites in the cyclic molecule. The present study shows the remarkable coordinating properties of the PABA molecule, and illustrates its ability to achieve a suitable balance between the driving force to coordinate to aminia binding sites of the cyclic molecules and its tendency to self-assemble *via* supramolecular heterosynthons in the structure of the complexes described herein.

The proton transfer within the complex seems to be a favorable factor for aquation, while in the case of the less polar classic O-containing crown ethers the anhydrous adducts have been obtained.[5] In the light of the hot paper[34] addressed to the important factors crucial for the organic crystal hydrates formation, the following generalizations for the studied system PABA–macrocycle could be highlighted. Survey of the hydrogen-bonding arrays easily reveals the significant role of water molecules to balance the number of proton-donor and proton-acceptor sites involved in the intermolecular hydrogen bonding interactions. In all supramolecular associates excluding **2** the sum of proton–acceptor sites for PABA and heterocyclic molecule exceeds the sum of proton-donors, and water molecules compensate this misbalance. Our study shows that the degree of such misbalance correlates with a number of water molecules included in the supramolecular associate. The largest disagreement between the number of H-donors and H-acceptors was found in trihydrate **5**, while only one water molecule per formula unit is involved in the supramolecular associate **2**, where the system PABA-heterocycle reveals a balance of H-binding sites. Thus, the reported crystal structures obviously show the important glue water function, which in all cases serves as an intermediate between the supramolecular reagents.

Acknowledgements

This study is supported by MRDA (Moldova)–CRDF (U.S.) award No. MRDA-008:BGP-III, MOC2-3063-CS-03.

References

1 (*a*) P. J. Osgood, S. H. Moss and D. J. Davies, *J. Invest. Dermatol.*, 1982, **79**(6), 354; (*b*) T. Sahr, S. Ravanel, G. Basset, B. P. Nichols, A. D. Hanson and F. Rebeille, *Biochem. J.*, 2006, **396**(1), 157; (*c*) O. Kornfeld and B. P. Nichols, *FEMS Microbiol. Lett.*, 2005, **251**(1), 137; (*d*) L. M. Elandalloussi, P. M. Rodrigues, R. Afonso, R. B. Leite, P. A. Nunes and M. L. Cancela, *Mol. Biochem. Parasitol.*, 2005, **142**(1), 106; (*e*) I. Meneau, D. Sanglard, J. Bille and P. M. Hauser, *Antimicrob. Agents Chemother.*, 2004, **48**(7), 2610; (*f*) J. Berglez, P. Iliades, W. Sirawaraporn, P. Coloe and I. Macreadie, *Int. J. Parasitol.*, 2004, **34**(1), 95; (*g*) L. A. Castelli, N. P. Nguyen and I. G. Macreadie, *FEMS Microbiol. Lett.*, 2001, **199**(2), 181; (*h*) P. Wang, P. F. Sims and J. E. Hyde, *Parasitology*, 1997, **115**(Pt 3), 223; (*i*) K. Yamasaki, T. Maruyama, U. Kragh-Hansen and M. Otagiri, *Biochim. Biophys. Acta*, 1996, **1295**(2), 147; (*j*) C. B. Lalor, G. L. Flynn and N. Weiner, *J. Pharm. Sci.*, 1994, **83**(11), 1525; (*k*) L. Ma, C. Ramachandran and N. D. Weiner, *J. Pharm. Sci.*, 1992, **81**(11), 1104.
2 M. C. Etter and G. A. Frankenbach, *Chem. Mater.*, 1989, **1**, 10–12.
3 M. Alleaume, G. Salas-Cimingo and J. Decap, *C. R. Acad. Sci., Ser. C*, 1966, **262**, 416.
4 A. Elbasyouny, H. J. Brugge, K. Deuten, M. Dickel, A. Knohel, K. U. Koch, J. Kopf, D. Melzer and G. Rudolph, *J. Am. Chem. Soc.*, 1983, **105**, 6568.
5 M. S. Fonari, Yu. A. Simonov, J. Lipkowski, A. A. Dvorkin and E. V. Ganin, *Supramol. Chem.*, 1994, **4**, 43.
6 C. M. Zakaria, A. J. Lough, G. Ferguson and C. Glidewell, *Acta Crystallogr., Sect. B: Struct. Sci.*, 2004, **60**, 65.
7 S. S. Basok, G. Bocelli, M. S. Fonari, E. V. Ganin and Yu. A. Simonov, *Acta Crystallogr., Sect. C: Cryst. Struct. Commun.*, 2006, **62**, o50.
8 F. H. Allen, *Acta Crystallogr., Sect. B: Struct. Sci.*, 2002, **58**, 380–388.

9 T. F. Lai and R. E. Marsh, *Acta Crystallogr*., 1967, **22**, 885.
10 S. Gracin and A. Fischer, *Acta Crystallogr., Sect. E: Struct. Rep. Online*, 2005, **61**, o1242.
11 R. M. Fuquen, R. H. De A. Santos and J. R. Lechat, *Acta Crystallogr., Sect. C: Cryst. Struct. Commun*., 1996, **52**, 220.
12 D. E. Lynch, G. Smith, K. A. Byriel and C. H. L. Kennard, *J. Chem. Soc., Chem. Commun*., 1992, 300.
13 G. Smith, K. E. Baldry, K. A. Byriel and C. H. L. Kennard, *Aust. J. Chem*., 1997, **50**, 727.
14 K. A. Byriel, D. E. Lynch, G. Smith and C. H. L. Kennard, *Aust. J. Chem*., 1991, **44**, 1459.
15 R. Moreno-Fuquen, M. Font i Carot, M. Garriga, F. Cano, M. Martinez-Ripoll, J. Valderrama-Naranjo and M. L. Serratto, *Acta Crystallogr., Sect. E: Struct. Rep. Online*, 2003, **59**, o495.
16 J. A. McMahon, J. A. Bis, P. Vishweshwar, T. R. Shattock, O. L. McLaughlin and M. J. Zaworotko, *Z. Kristallogr*., 2005, **220**, 340.
17 Ruihu Wang, Feilong Jiang, Youfu Zhou, Lei Han and Maochun Hong, *Inorg. Chim. Acta*, 2005, **358**, 545.
18 J. R. Bowers, G. W. Hopkins, G. P. A. Yap and K. A. Wheeler, *Cryst. Growth Des*., 2005, **5**, 727.
19 See, for example, besides already mentioned: D. E. Lynch and I. McClenaghan, *Acta Crystallogr., Sect. C: Cryst. Struct. Commun*., 2001, **57**, 830.
20 G. Smith, K. A. Byriel and C. H. L. Kennard, *Aust. J. Chem*., 1999, **52**, 625.
21 D. E. Lynch, G. Smith, D. Freney, K. A. Byriel and C. H. L. Kennard, *Aust. J. Chem*., 1994, **47**, 1095.
22 G. Smith, D. E. Lynch, K. A. Byriel and C. H. L. Kennard, *Aust. J. Chem*., 1995, **48**, 1133.
23 G. Smith, U. D. Wermuth and J. M. White, *Acta Crystallogr., Sect. E: Struct. Rep. Online*, 2005, **61**, o313.
24 V. O. Gelmboldt, A. A. Ennan, E. V. Ganin, Yu. A. Simonov, M. S. Fonari and M. M. Botoshansky, *J. Fluorine Chem*., 2004, **125**, 1951.
25 Z. J. Li, Yu. Abramov, J. Bordner, J. Leonard, A. Medek and A. V. Trask, *J. Am. Chem. Soc*., 2006, **128**, 8199.
26 S. G. Fleischman, S. S. Kuduva, J. A. McMahon, B. Moulton, R. D. B. Walsh, N. Rodriguez- Hornedo and M. J. Zaworotko, *Cryst. Growth Des*., 2003, **3**, 909.
27 P. Vishweshwar, J. A. Mcmahon, J. A. Bis and M. J. Zaworotko, *J. Pharm. Sci*., 2006, **95**, 499.
28 G. M. Sheldrick, *SHELXS and SHELXL97 Programs for structure refinement and solution*, Göttingen, Germany, 1997.
29 SADABS (Area Detector Absorption Correction), Siemens Industrial Automation, Inc, Madison, WI, 1996.
30 (*a*) M. C. Etter, *Acc. Chem. Res*., 1990, **23**, 120; (*b*) J. Bernstein, R. E. Davis, I. Shimoni and N.-L. Chang, *Angew. Chem., Int. Ed. Engl*., 1995, **34**, 1555.
31 (*a*) M. S. Fonari, V. Ch. Kravtsov, Yu. A. Simonov, S. S. Basok and E. V. Ganin, Supramolecular architecture in the co-crystals of azacrown ethers with salicylic acid, in *Moldavian–Polish–Ukrainian Symposium on Supramolecular Chemistry*, Chisinau, Moldova, October 10–12, 2005, Abstracts, p. 65.
32 (*a*) T. M. Krygowski, S. J. Grabowski and J. Konarski, *Tetrahedron*, 1998, **54**, 11311.
33 (*a*) A. L. Gillon, N. Feeder, R. J. Davey and R. Storey, *Cryst. Growth Des*., 2003, **3**, 663.
34 (*a*) L. Infantes, L. Fábián and W. D. S. Motherwell, *Cryst EngComm*, 2007, **9**, 65.

